



ELSEVIER

Marine and Petroleum Geology 21 (2004) 933–946

Marine and
Petroleum Geology

www.elsevier.com/locate/marpetgeo

Modelling approaches to understanding fold development: implications for hydrocarbon reservoirs

Martin Casey*, Robert W.H. Butler

School of Earth Sciences, Leeds University, Leeds LS2 9JT, UK

Received 31 March 2003; received in revised form 16 December 2003; accepted 3 January 2004

Abstract

A mechanics-based approach to the evolution of buckle folds is proposed. Existing analytic and simple numerical models are used to demonstrate that dramatic changes in layer parallel stress occur in developing folds and that the bulk effective rheology of folding rocks is strongly reduced in relation to neighbouring rocks with no folds. A methodology for estimating regions of folds more or less likely to suffer fracture is set out. In this methodology a simple abstraction of the natural fold is identified and the stress history during its development is calculated using linear viscosity as a proxy for competence. This simple and computationally cheap approach allows all salient features of natural multilayer folds to be recreated in numerical experiments. The final step in the method is to use the stress conditions for three types of fracture failure, tensile failure, dilatant shear failure and grain crushing to define potential functions that indicate increased or decreased probability of failure. Results give predictions that agree well with observation in the simple cases studied. A novel method for approximating three-dimensional deformations is used to model the propagation of folds in the axial direction and it is found that this occurs rapidly and allows constructive and destructive interference of propagating folds below a certain amplitude. This provides a means by which perturbations may interact over a certain distance. Such a mechanism was an implicit requisite of classic fold theories, but its identity has been obscure for three decades. It is shown that many small perturbations are needed to give patches of coherent folds and that few, large perturbations give single arc folds.

© 2004 Elsevier Ltd. All rights reserved.

Keywords: Hydrocarbon reservoirs; Rock fracture; Multilayer folds

1. Introduction

Folds are host to many hydrocarbon reservoirs in diverse tectonic settings. The purpose of this paper is to examine the application of mechanical approaches to predict the development of buckle folds the better to assess not only the bed-scale damage within reservoir units but also to understand the three-dimensional evolution of fold trains.

Bed-scale damage can play a critical role in the performance of hydrocarbon reservoirs through modification of the porosity and permeability of the original rock. It has long been recognised that this damage can have a variable impact. Simple open fractures may enhance permeability but grain crushing and clay smear can create permeability barriers. Further, the timing of damage events relative to the diagenetic history is critical in determining

the long-term character of the damaged bed and even its response to progressive deformation. Much of this may be difficult to resolve in the subsurface although these features are well understood from outcrop studies. Given these complexities, there are increasing attempts to relate bed-scale damage to the larger-scale structure that might be resolved on seismic data.

Many attempts take a kinematic approach whereby the final geometry or the inferred geometric evolution of a fold is used to predict fracture damage within beds. Outcrop studies have tested this approach with varying degrees of success. For example, Hennings, Olson and Thompson (2000) studied jointing patterns, inferred to be tectonically produced fractures, around a broad anticline related to a basement-involved structure in Wyoming. The intensity of damage correlated reasonably well with the finite curvature of beds. Contrast this result with that of Jamison (1997), working on an anticline in the foothills of the Canadian Rockies, using mineralised extension veins as proxies for

* Corresponding author. Fax: +44-113-233-5259.

E-mail address: m.casey@earth.leeds.ac.uk (M. Casey).

fractures in the subsurface. On the backlimb of the structure the strikes of extension fractures were parallel to the large-scale fold hinge. However, the fractures on the forelimb showed highly variable orientations. Furthermore, there was no correlation in the intensity or aperture of fractures with structural position. In yet another example, Hanks, Lorenz, Teufel and Krumhardt (1997) in their study of damage in the Lisburne Group of the Brooks Range, Alaska, found that a key control on the orientation and intensity of fracture, mineralised and open, late joints, was lithology. They also suggested that flexural slip was the key mechanism of large-scale folding that influenced bed-scale damage, a conclusion supported by the work of Couples and Lewis (1998) elsewhere. For these workers we can infer that fold limbs are likely to show greater strain, and therefore more bed-scale damage than the hinge areas of folds. If correct then curvature is likely to be of subordinate importance to interlimb angle and, for upright folds, its proxy of bed-dip.

The lack of a clear picture might suggest an alternative approach to the problem. The papers cited above all report the results of field studies where the deformation is the final finished product of the deformation history. Yet the fracture processes affecting reservoir quality and fluid flow properties are mostly the result of particular stress conditions and may not in themselves account for a large amount of finite strain. Consequently we propose an approach based on estimates of the stress history of folding to gain an indication of when and where fracture processes may occur.

Fracture embraces only part of the possible array of deformation mechanisms in rocks. The presence of syntectonic mineralisation along fracture points to accompanying dissolution–reprecipitation processes operating in tandem with cataclasis. These processes will make an important contribution to the rheological properties of the rock which can be represented by the field term ‘competence’.

There are key differences in the finite pattern of damage associated with buckle folds and forced folds, as discussed by Cosgrove and Ameen (2000). The general style of the fracture pattern associated with buckle folds is discussed by Price and Cosgrove (1990) but the timing and evolution of fracture arrays are less well-understood. Many workers suggest that the primary control on fracture density in folds, regardless of the type of folding, is curvature (e.g. Lisle, 1992). However, other variables play a role, such as lithology (e.g. Ericson, McKean, & Hooper, 1998).

Many compressional terrains show evidence for widespread development of buckle folds (e.g. the Zagros deformation belt of Iran; Satterzedah, Cosgrove, & Vita Finzi, 2000) where folding is the response to end loading of originally subhorizontal layering. Geometrically this style of deformation, when decoupled mechanically from underlying basement, has also been termed ‘detachment folding’. There are numerous recent accounts of detachment

folding, reviewed by Mitra (2002), where the large-scale structural geometry, e.g. wavelength, is discussed principally in kinematic terms. However, previous studies of buckle folds emphasise the importance of geometric variables together with rheological parameters, such as competence contrast, in fold development. Therefore to understand not only the large-scale evolution of fold belts but also the consequences of deformation, such as fracture patterns and fracture density, demands a mechanical approach.

Fold development has been studied using analytical solutions (Biot, 1961; Fletcher, 1974; Ramberg, 1960; Smith, 1977), physical analogue models (Cobbold, 1975; Mancktelow & Abbassi, 1992) and numerical methods (Cobbold, 1977; Dieterich & Carter, 1969; Williams, 1980). The analytical approaches are valid for the initial phases of folding and provide understanding of how wavelength and rate of growth of folds are related to the physical properties of the rocks. The development of folds to finite amplitude can be studied by physical analogue models or numerical methods. Both physical analogue models and numerical modelling show how the geometric forms of folds evolve with increasing applied strain, but only numerical models give quantitative results for such things as the stress evolution.

A description of buckle folding is presented below. First a summary of the classic analytical buckling theory is outlined and some important results cited. These results are applied and extended by numerical studies, which aim principally to understand the mechanics of finite amplitude fold development. This part of the paper consists of two themes:

- (1) Deriving the stress history of folding as an aid to finding areas of increased fracture likelihood.
- (2) Understanding the way in which folding rock masses interact with rocks without folds or with faults.

2. Analytical fold theories

First we will review some results from analytical fold theories, which make great simplifications in the geometry of folds studied but which come to some fundamental and significant results. The analytical fold theories of Biot (1961) and Ramberg (1960) investigate the conditions under which folds form in a single stiff layer embedded in a less stiff matrix. They find that in order for folds to grow there must be small amplitude initial perturbations of the layering and that a perturbation of a given wavelength and amplitude A_0 will grow according to $A = A_0 \exp(\alpha\epsilon)$, where A is the amplitude after a strain of ϵ has been applied and α is a constant. Low values of alpha give a slower growth of the fold, higher values give a higher rate, but there is always an ever increasing rate of growth of the fold with applied strain which is determined by the exponential function. It is

the exponential nature of fold amplitude growth that distinguishes it from passive folding, such as fault-bend folding associated with thrust ramps. Mechanically it means that the driving force of folding increases with the amplitude of the fold.

The constant alpha is a function of both the contrast in stiffness between the layer and its matrix and the wavelength. There is a particular wavelength for which alpha has a maximum and from which it falls quite sharply to longer and shorter wavelengths. In the classic fold theory it is postulated that all wavelengths are present as initial irregularities in the layer, but that only those close to the maximum are amplified significantly quickly so that the result after a finite deformation is folds close to that wavelength, called the dominant wavelength. This postulate implies that there is a means by which perturbations can communicate over a distance in the rock so that they can interfere constructively and destructively to give a coherent patch of folds in the rock. This means of communication is one of the themes of this paper and a possible candidate is presented below.

In addition to folds developing in a single layer in a less stiff matrix, there are other mechanical situations that lead to folding governed by an exponential growth of amplitude with applied strain. Two examples are the folding of sequences of alternating stiff and less stiff layers in an approximately similar manner and the development of folds within a layer of homogeneous, anisotropic material. The former example is very useful in natural folds as most sedimentary rock sequences approximate to sequences of strong and weak rocks: sandstones and shales in turbidites or alternations of limestones and marls in the Mesozoic of the Alpine–Himalayan belt, e.g. the Zagros mountains. There exist analytical solutions for these cases also (e.g. Biot, 1965) and the solutions are very similar to those for single layers.

3. Simple numerical models of folds

The insights gained from analytical solutions can be extended to finite amplitude folds by carrying out some simple numerical modelling. The work reported here uses the finite element method, a few technical details of which are given in Appendix A, to calculate the instantaneous deformation in a simplified geometrical model of a fold. Fig. 1 shows the development of a fold profile calculated using the finite element method. The successive profiles show an evolution of shape from the original sinusoid to a shape with straight limbs and sharp hinges as the amplitude increases. The dashed line in Fig. 1 is the locus of the crest or hinge point of the fold calculated on the basis of the initial exponential growth as predicted by the analytical approach and confirmed by numerical modelling for the early stages of the run. The exponential growth locus deviates from the actual locus at the point where further exponential growth

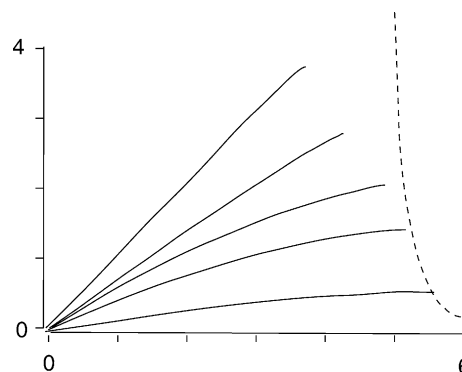


Fig. 1. Development of a fold profile in an internal buckle. The profiles are quarter wavelength portions of the fold from inflexion point on the limb located at the origin of the graph to the hinge point at the right. The lowest profile is the initial sinusoidal fold and the higher curves show the shape at successive steps of imposed deformation. The dashed curve on the left is the locus of the hinge line for a continuous exponential growth.

would lead to extension of the arc of the fold. Results of several runs of varying exponential growth rates, showing just the hinge point loci, are shown in Fig. 2. The actual profiles have been left out to avoid cluttering the diagram. They all show the same evolutionary trend as the profile of Fig. 1. The more weakly developing folds have a greater amount of layer shortening and a longer exponential growth phase than the more strongly developing folds. The dashed lines in Fig. 2 are arcs centred on the inflexion point, which is located at the origin of the diagram. It can be seen that the loci of the hinge lines tend to run parallel to the arcs after the exponential stage is over. This means that in this stage of the fold development the limbs of the fold are rotating as if the fold hinges were behaving as door hinges. The limbs simply rotate with no length change and the hinges bend. This behaviour was assumed to occur at all stages of fold development in the model of Ramsay (1974).

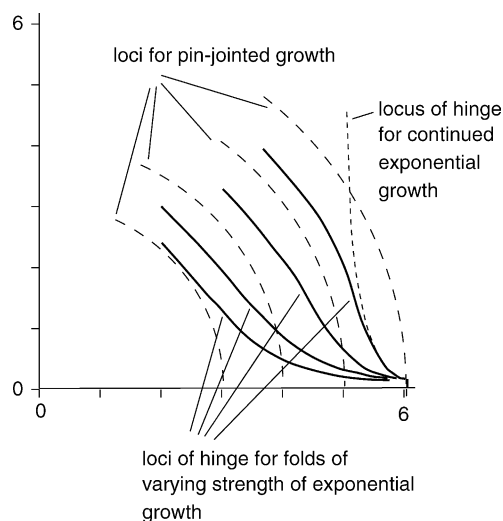


Fig. 2. The thick lines are the loci of hinge points for several fold simulations with varying strengths of exponential growth. The long-dashed lines are arcs on the origin of the graphs, which is also the inflexion points of the fold profiles.

In summary, these results indicate that at low amplitude the fold limbs are shortened, but that this shortening becomes less and less as the fold shape evolves to that of a chevron fold. It will be shown later that this transition takes place with a very sharp reduction in compressive stress parallel to the layering. Mechanically the fold instability comes from a progressive transfer of strain from layer parallel shortening to layer parallel shear. As the fold amplitude increases the way in which a bulk shortening can be taken up by layer parallel shear becomes more and more favourable: hence the exponential nature of the fold growth.

3.1. Methodology for predicting fracture

The use of numerical models to predict areas of deformed rocks that are more prone to fracture requires a carefully devised procedure. For our studies we have followed a three-stage protocol:

- (1) The identification of a simplification of nature that is sufficiently complex to capture the essential behaviour, but sufficiently simple to be realised.
- (2) Use the simplification to calculate stress distributions.
- (3) Take the stress distributions and apply them to rocks with brittle deformation behaviour.

These steps will be applied to the problem of identifying fracture prone regions in rock sequences consisting of alternations of more and less competent rock layer in the next three sections.

3.2. Simplifying nature

Most natural active buckle folds occur in alternating sequences of more and less competent rock layers. A further simplification comes from the observation that fold amplitude and profile shape vary very slowly with distance along the axial plane and the folds can be approximated as similar folds without loss of accuracy, see for example, Casey and Huggenberger (1985). As the folds develop the growth of amplitude allows the shortening deformation, initially parallel to the layers, to be taken up by shearing of the incompetent material. This is the flexural slip or flexural flow mechanism of Ramsay (1967). Consequently the fold development in this situation can be modelled by considering the deformation of two layers of different Newtonian viscosity with periodic boundary conditions on the mid-line of one of the units, see Appendix A for details. It is certain that the rheology in nature is not linear viscous, but models on this basis are able to reproduce the shapes and finite strain patterns of natural folds (Williams, 1980). The important feature is that one layer is hard to deform and supports a high stress while the other is easy to deform. This strength variation must exist regardless of the rheological simplification used for modelling.

3.3. Stresses in multilayer folds

Using the model abstraction presented in the previous section the finite element method can be used to model the growth of finite amplitude folds from small initial perturbations. The values of the principal stresses and their orientations can then be calculated at all points in the model at each stage of the deformation. The technical details are presented in Appendix A. Results are presented below for various steps in the deformation. Constant strain rate is imposed on the bulk region containing the folds. Each step in the solution corresponds to a time interval and the strain accumulated is given by:

$$\epsilon = d\Delta t \quad (1)$$

where ϵ is natural strain, d is the imposed differential strain rate and Δt is the time interval. The natural strain defined by $\epsilon = \ln(l/l_0)$ where l is the strained length and l_0 is the unstrained length. Each step corresponds to the imposition of a differential natural strain of 0.1 on the boundaries, where the differential natural strain is the difference of the extensional natural strain in y and the shortening natural strain in x .

3.4. Rock fracture and its application to the stress results

As a preliminary to a more detailed exploration of stress histories in folding the relationship between stress and rock fracture will be outlined, see Paterson (1978). The simplest way a rock can fracture is by tensile failure. For this to occur in the subsurface the pore pressure must exceed the least principal stress. A function of stress which indicates potential for tensile fracture, or for the opening of existing fracture planes is the least principal stress. For compressive brittle failure functions of both principal stresses are needed. Fig. 3 is a simplification of the failure envelope for porous

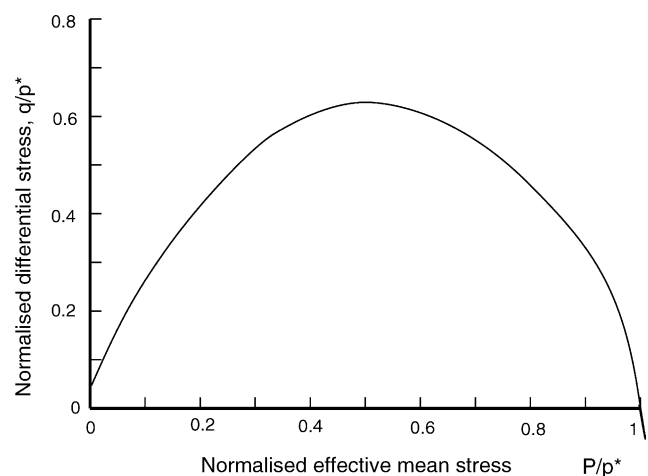


Fig. 3. Simplified failure envelope for porous rocks. The graph is a plot of normalised differential stress against normalised effective pressure. The failure line rises at low P/p^* , reaches a maximum and then falls. Simplified from Wong et al. (1997).

rocks, taken from Wong, David and Zhu (1997). The graph is normalised differential stress against normalised effective pressure, which is the actual confining pressure minus the pore fluid pressure. The normalisation factor, p^* , is the crushing strength of the rock in the absence of differential stress. At low values of confining pressure there is a positive dependence of failure strength and confining pressure and the mode of failure is dilational. This mode of failure is the same as that for dense rocks with microcracks. At high confining pressures the strength decreases with increasing confining pressure, the failure is compactional and is dominated by crushing of grains as a result of high point contact loads. The fracture of rocks in natural deformations is extremely difficult to predict, as it depends on many irregularities in the deformation, such as, among others,

variations in pore pressure or local heterogeneities in rock properties. Consequently it is sought here to give an indication of the tendency of the rock to fracture as a function of stresses calculated from continuum models. This is achieved by defining fracture potential functions which will give an indication of likelihood of fracture. One potential function is defined for the low confining pressure portion of Fig. 3. Using data from Paterson (1978) the following function is defined:

$$\text{Pot} = 4.5 \text{ differential stress} - 5 \text{ mean stress} \quad (2)$$

This function increases to the upper left of the plot in Fig. 3.

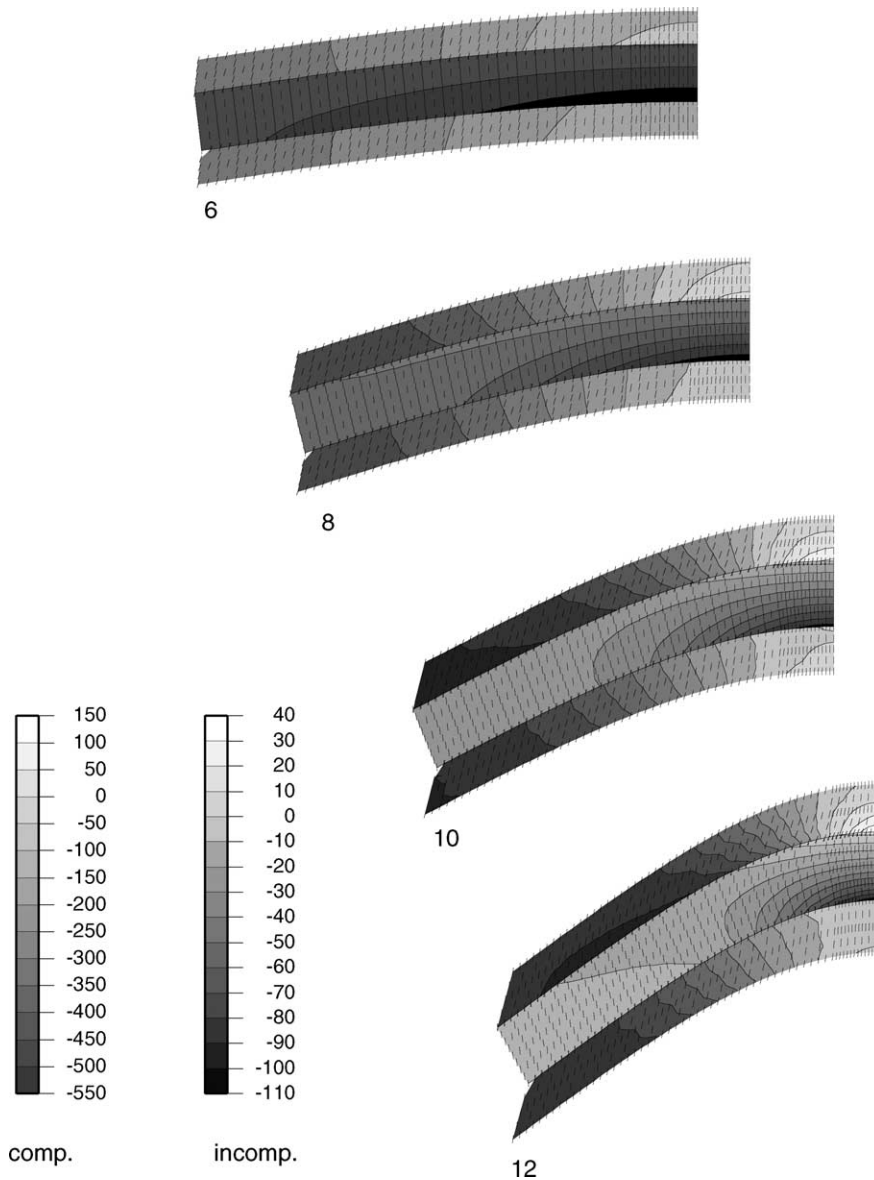


Fig. 4. The value of the most compressive principal stress for steps in the development of a multilayer similar fold with a viscosity ratio of 10. One quarter of the wavelength is shown and the top of each picture continues on the bottom. The competent layer is in the middle. The short lines give the orientation of the least compressive principal stress. The numbers against each picture give the number of steps in the model. The stress scales are given nominally in Megapascals.

The potential for compactional failure is defined as

$$\text{Pot} = \text{differential stress} + \text{mean stress} \quad (3)$$

This function increases to the top right of Fig. 3.

Results of computations are shown in Figs. (4)–(9). Fig. 4 shows the development of the most compressive principal stress for the model with a viscosity ratio of 10. This stress is the compressive stress which acts parallel to the layer boundaries and is the main driving force of the folding instability. The most striking feature of the development of this stress with fold growth is the strong fall of stress in the competent layer from in excess of 500 Units in step 6, through 350 Units in step 8, 200 in step 10 to 100 in step 12. In fact, the main fall occurs before step 6. This is a consequence of the exponential growth of the fold changing the mode from layer parallel shortening to pin-jointed behaviour. In a general layered stack of rocks the amplitudes of folds varies up and down the axial plane trace in the profile section. If the competent/incompetent layer pair under consideration were the one in which the amplitude developed quickest, the fall in layer parallel compressive stress would result in load transfer to the rocks in the lower amplitude folds, accelerating fold growth or promoting brittle shear failure to cause thrusting. For the competent

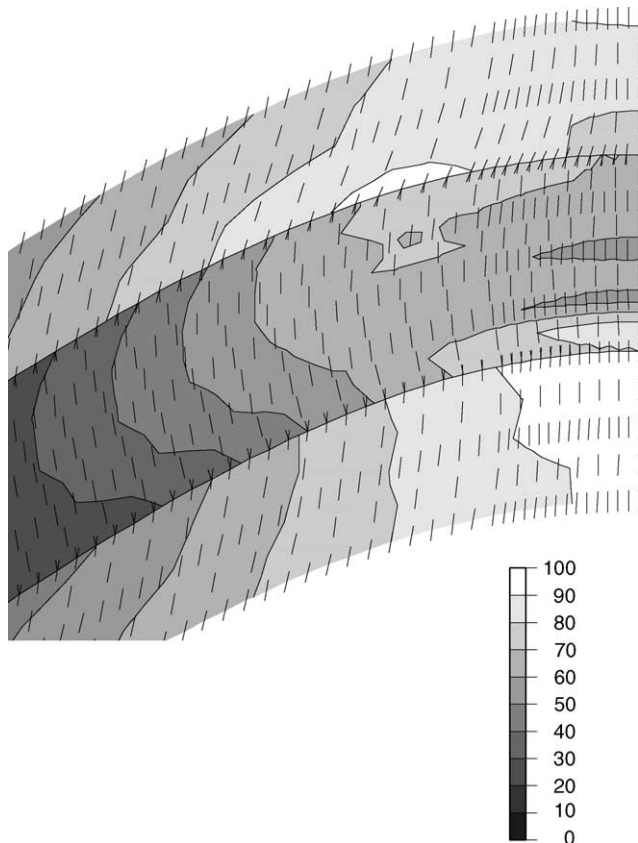


Fig. 5. The value of the least compressive principal stress for step 12 in the development of a multilayer similar fold with a viscosity ratio of 10. Details of stresses in the hinge region. Tensile failure is most probable in the incompetent unit with layer parallel fracture.

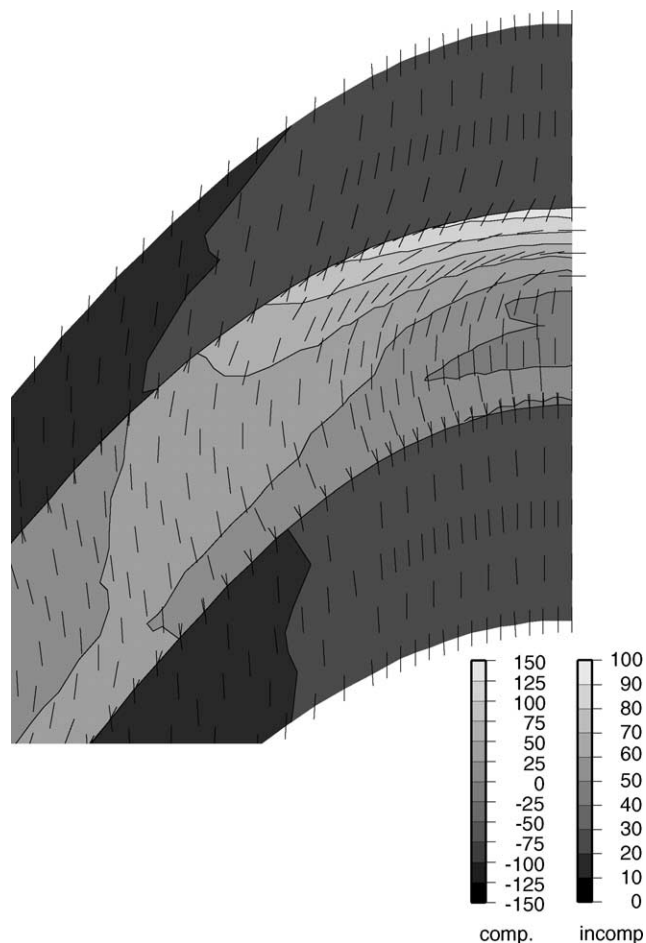


Fig. 6. The value of the least compressive principal stress for step 12 in the development of a multilayer similar fold with a viscosity ratio of 40. Details of stresses in the hinge region. The most probable location of fracture is on the outer arc of the competent layer with the fractures perpendicular to layering.

unit, layer parallel stress remains high in the inner arc of the hinge, which becomes progressively narrower with imposed strain. This will tend to give shear failure in the inner arc, as discussed below. In the incompetent unit the compressive stress shows a trend from more compressive in the limb to less compressive in the hinge. This is a consequence of material being squeezed out of the limb and into the hinge. This effect becomes stronger with increasing limb dip and it is caused by space problems in the limb area: the vertical extensional strain in the competent layer comes from its simple rotation about the inflexion points, with minimal internal strain. This strain rate soon becomes greater than that required for both competent and incompetent unit and hence the incompetent material is expressed. The variation of compressive stress reflects the variation in pressure consequent on the transport of incompetent material to the hinge.

Fig. 5 shows the variation of the less compressive principal stress for a viscosity ratio of 10 in the hinge region for a multilayer fold of viscosity ratio 10. This stress component acts perpendicular to the layer boundary and its

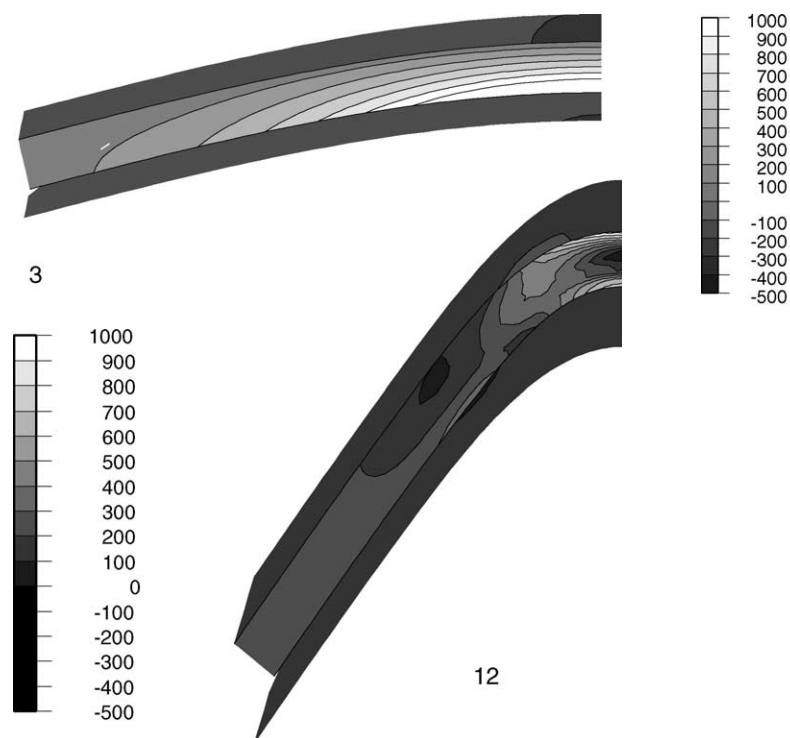


Fig. 7. The value of the fracture potential for steps 3 and 12 in the development of a multilayer similar fold with a viscosity ratio of 40. One quarter of the wavelength is shown and the top of each picture continues on the bottom. The competent layer is in the middle. The numbers against each picture give the number of steps in the model. The stress scales are given nominally in Megapascals, but the absolute values are not very meaningful. Higher positive values of this function of stress, the fracture potential, indicate a greater likelihood of shear failure. Failures would occur in conjugate sets at plus and minus 30° to the layering, except in the outer arcs of the hinges, where they would be at plus and minus 60° to layering.

behaviour is almost completely determined by the extrusion process described in the last paragraph. The general level of this stress component in the competent unit is less tensile than in the incompetent unit. This is the effect on the mean stress of the high value of the more compressive stress. The highest value occurs in the incompetent unit on the inner arc of the hinge and it gives a tendency to produce fractures parallel to the layer boundary.

Fig. 5 also shows the effect of bending the competent unit, but only in the outer three-quarters of the layer: the stress goes from around 50 Units at one-quarter height from the inner arc to around 65 Units at the outer edge. The stress in the lower quarter of the layer is determined by the high value in the incompetent unit. Detail of the distribution of the least compressive principal stress for a multilayer with a viscosity ratio of 40 is shown in Fig. 6. The picture is dominated by the strong maximum at the outer arc of the hinge, showing a tendency to form tensile fractures perpendicular to the layering, i.e. perpendicular to the lines giving the line of action of the least compressive principal stress. The value of this stress component in the incompetent unit is a consequence of extrusion of

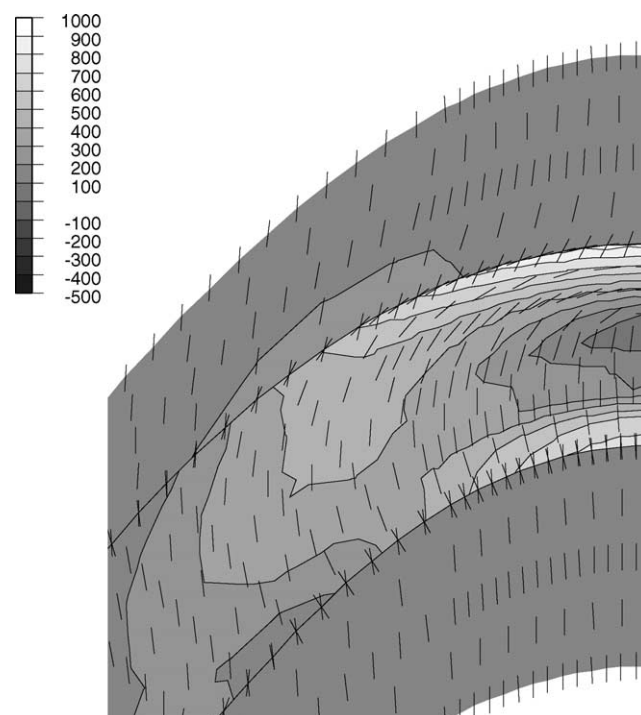


Fig. 8. The value of the fracture potential for step 12 in the development of a multilayer similar fold with a viscosity ratio of 40. Details in the hinge region.

incompetent material from limb to hinge. As in the case of the model with a viscosity ratio of 10 the least compressive stress on the inner arc of the fold is also made more positive by the effect of the incompetent unit value.

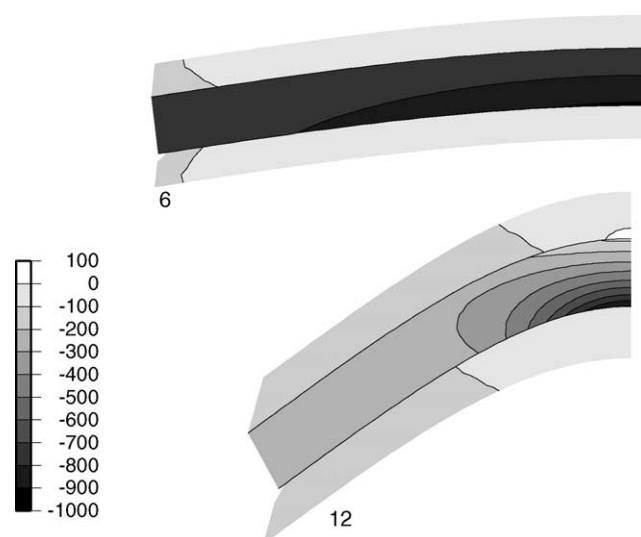


Fig. 9. The value of the crushing failure potential function of Eq. (2) for steps 6 and 12 in the development of a multilayer similar fold with a viscosity ratio of 10. One quarter of the wavelength is shown and the top of each picture continues on the bottom. The competent layer is in the middle. The short lines give the orientation of the least compressive principal stress. The numbers against each picture give the number of steps in the model. The stress scales are given nominally in Megapascals, but the absolute values are not very meaningful. Higher negative values of this function of stress indicate a greater likelihood of grain crushing failure.

Values of the fracture potential function of Eq. (2) are shown in Fig. 7 for the multilayer model with a viscosity ratio of 40. The value is dominated by the high layer parallel compressive stress in the early stages and develops maxima both on the inner and on the out arc in later stages when the bending of the hinge becomes strong. Detail of the hinge area is shown in Fig. 8. The shear failure planes lie at plus and minus 60° to the direction of the least compressive principal stress as given by the short lines in Fig. 8. Thus thrust faulting will form in the inner arc and normal faulting in the outer arc.

Fig. 9 shows the variation of the potential function for crushing failure of Eq. (2) for steps 2 and 12 in the development of similar multilayer folds for a viscosity ratio of 10. A value for the normalising factor p^* has not been incorporated into the plot and the low stresses of the incompetent layer suggest that crushing would not occur there. The values in the competent unit are dominated by the value of the layer parallel compressive stress shown in Fig. 4. The high values of this component in the low amplitude steps indicates a strong tendency to crushing failure in a large proportion of the layer at these stages with a concentration in the inner arc at higher amplitudes. A constant end load boundary condition would again reduce the tendency to distributed crushing at early stages, leaving crushing in the inner arc of the hinge as the main prediction of these results.

The main conclusions that can be drawn from these results is that bending of the hinge dominates in showing likely locations of fracture by tensile failure, brittle shear failure or grain crushing, an expected result considering that the stress distribution is almost the same as that for a bending beam. This further supports the importance of competent bed curvature as a determinant of the fracture distribution. This expected result can be used to validate the technique for its subsequent use in more complex situations such folds developing in rotational deformation histories and folds developing in interaction with faults. Some more subtle indicators come from such features as the extrusion of incompetent material in the low viscosity ratio case.

A very strong feature of these results is the very sharp reduction in the layer parallel stress as a fold grows in amplitude. This means that the bulk effective strength of folding rocks varies enormously and this has important consequences for the interaction of folding and, for instance, faulting as well as for stress effects of load transfer within fold packets.

4. Along axis propagation of folds

Mechanical modelling can also be applied to understand the large-scale evolution of folded terrains. In these situations it can be important to evaluate how folds interact in three dimensions—for example to assess the relative rates

of fold amplification and lateral propagation in the evolution of four-way closure. Furthermore the approach can yield insights on large-scale stress histories over the evolution of deformations that may in turn impact on assessments of dynamic fracture systems.

For example, the geomorphological study of the folding in the Zagros indicates that folds several wavelengths long nucleate and then grow by increase in amplitude and propagation along the axis. Propagation appears to stop when a packet of folds collides with a neighbour. Thus the understanding of the mechanics of the folding and the modelling of the stress history of units in the folds requires an understanding of the processes of nucleation and propagation. This study was undertaken approximating the folds as similar folds with vertical axial planes, subhorizontal axes, and of infinite extent in the vertical direction, forming in a material with anisotropic deformation properties. In this approximation the geometry of the folds can change in the horizontal dimension but folded surfaces separated from one another by vertical displacement have the same geometry. This symmetry can be exploited in the formulation of the finite element program, see Appendix A.

The classic folding theories of Biot and Ramberg envisage the development of a dominant wavelength by amplitude selection of the fastest growing wavelength from initial perturbations in which all wavelengths are present. This mechanism requires a means by which perturbations separated in space can interact. Cobbold (1977) and Hunt, Mühlhaus and Whiting (1997) propose that elastic effects are important in this process, but have not demonstrated that they are important in geological deformations with slow strain rates and low viscosity materials. One of the main motivations for the project reported here was to explore the possibility that interactions in the axial direction of folds can provide the means by which perturbations interact. Models were run with various values of the degree of anisotropy, m . A value of one third for m corresponds to an isotropic material. A value of m less than one third means that the material is easy to shear in the plane parallel to layering. The growth of amplitude with imposed strain follows the result from fold theory:

$$A = A_0 \exp(\alpha\epsilon) \quad (4)$$

where ϵ is the imposed logarithmic strain, α is a constant, A_0 is the initial amplitude and A is the current amplitude. The constant α depends directly on the degree of anisotropy of the material. The rate of propagation of an initial perturbation along the fold axis is shown in Fig. 10. A persistent profile is rapidly established. The profile consists of an exponentially rising portion in front followed by a more or less linear portion and finally a portion of progressively slower growth. Only the exponential portion will be considered further in this paper. The profile spreads along the layer very rapidly with imposed strain and with a rate dependent on the degree of anisotropy.

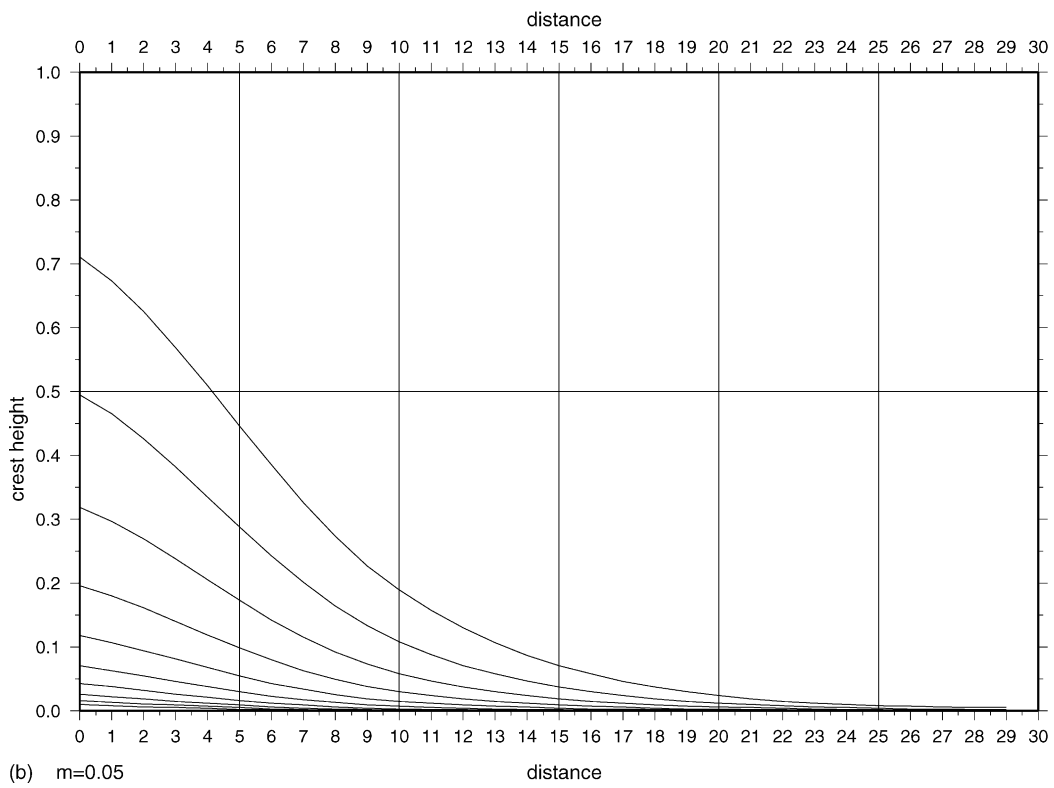
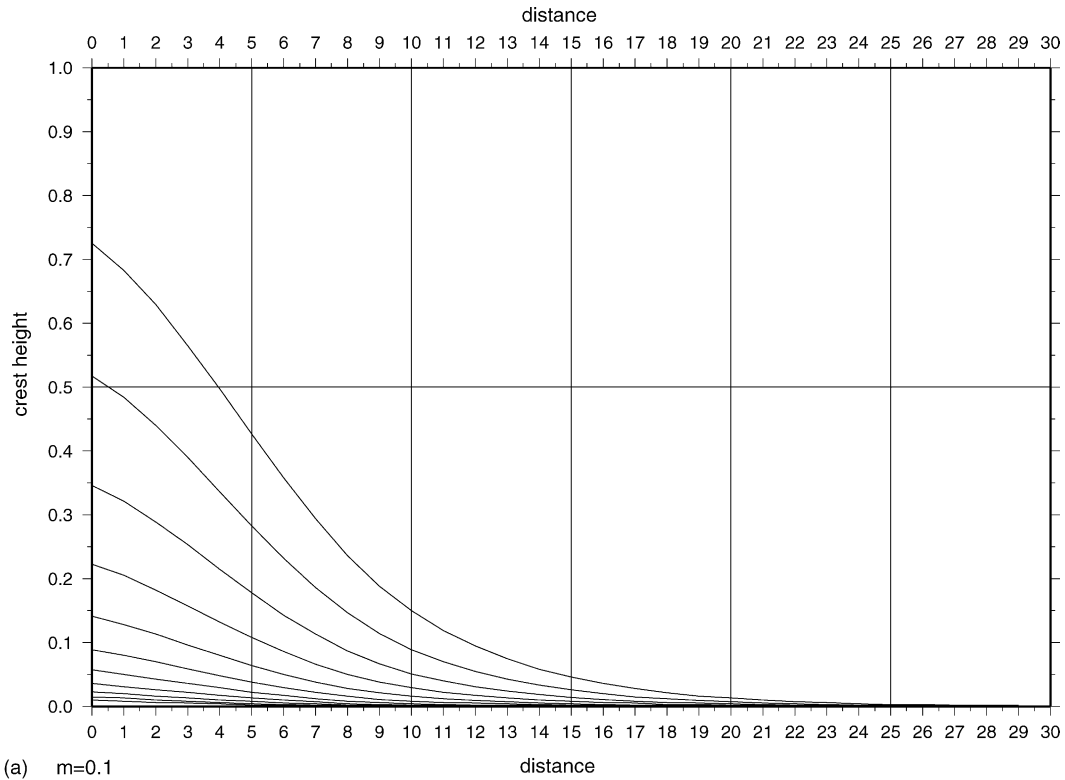


Fig. 10. Crest line profile of an anticline for two models runs. (a) anisotropy 0.1, step length 0.1, (b) anisotropy 0.05, step length 0.05.

Fig. 11 shows folds propagating towards one another with an offset of two units, that is, one fifth of a wavelength, for steps 4, 5, 6 and 8. In step 4 there is no perceptible interaction at the contour intervals chosen. In step 5

interaction becomes apparent in a bending away of the contour to meet the other fold. In step 6 a connecting ridge is being established which is clearly to be seen in step 8. The folds at the point where the amplitude is 0.2 for step 6 do not

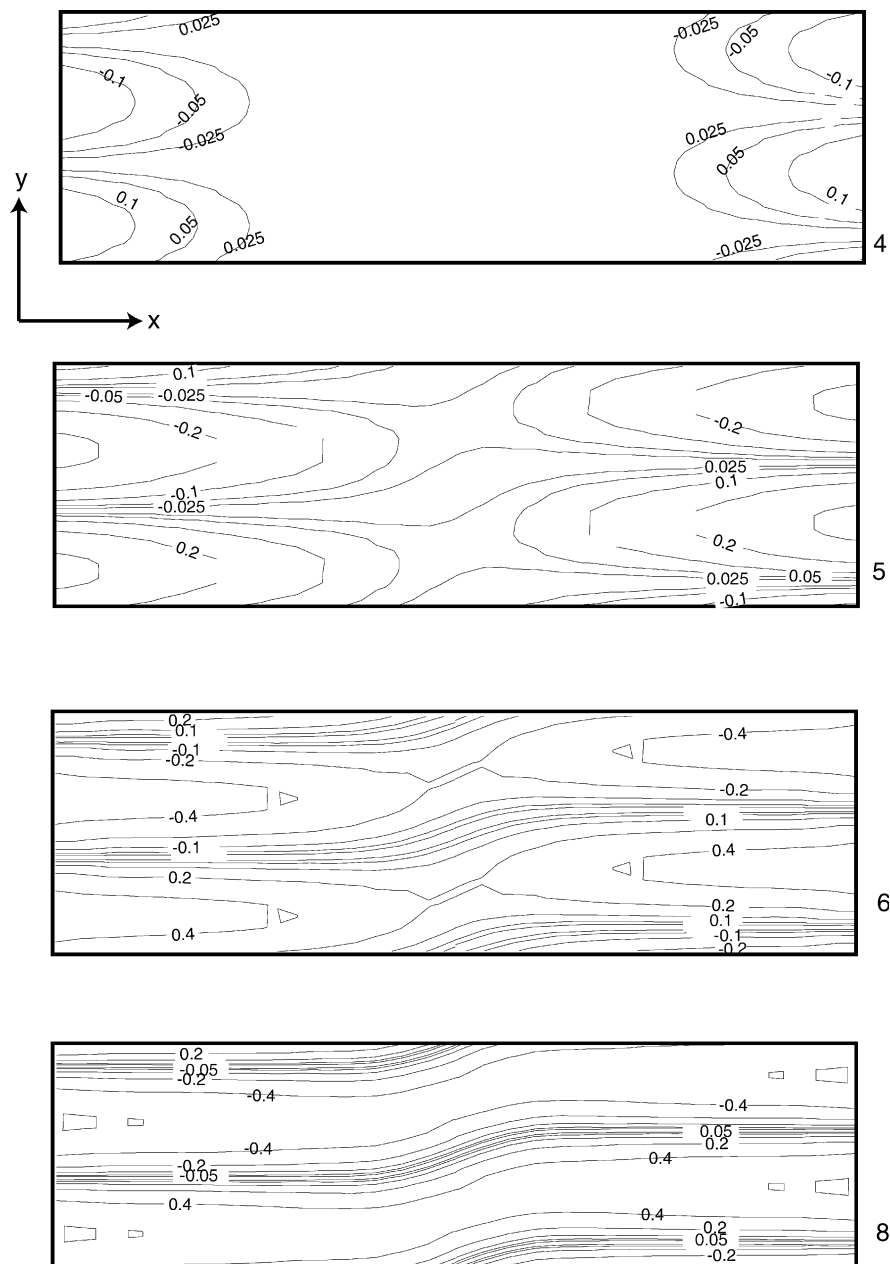


Fig. 11. Contour plot of fold development for a fold with anisotropy $m = 0.001$ and a layer thickness of n units. The numbers refer to step number and the steps are of 0.1 bulk logarithmic strain. The fold at the right hand side propagates left-wards with an offset of 2 units.

shift in their crest and trough lines in the subsequent history of the folding. This suggests that there is a cut off in amplitude for interaction. If we take this to be 0.2 on a wavelength of 10.0 this can be expressed as a cut-off amplitude to wavelength ratio of 0.02. The numerical experiments reported here can give some insight into the extent and nature of interaction between natural initial perturbations and allow a discussion of several interesting problems.

The result that the rate of growth of amplitude and the rate of propagation of a perturbation along the axis both depend on the degree of anisotropy means that the same perturbation will spread and grow in an identical manner

regardless of the degree of anisotropy. A consequence of this is that aspects of folding, such as the existence and size of coherent patches of folds, is not dependent on anisotropy. A further consequence is that the control on these aspects must be predominantly the initial perturbations. The interaction of folds reported above indicates the existence of an upper limit of amplitude to wavelength ratio for interaction. This means that interaction to establish coherent patches must occur between this level and the average size of the initial perturbations. If this interval spans many orders of magnitude the interaction can be long-range, so that folding of almost perfectly layered rocks or rocks with a regular fabric can be expected to have relatively large

volumes of coherent folds. On the other hand regions containing single anticlines would be expected to have a small number of large perturbations, such as syn-sedimentary faults. So the regularity of folding is an indicator of the perfection of layering before folding. Although the interaction of folds is independent of anisotropy, the amount of imposed strain required to achieve the interaction is still dependent on this parameter. As all the interaction is expected to take place below an amplitude to wavelength ratio of 0.02 the strain required will be recorded in the amount of layer parallel shortening observable in competent units.

The area in front of a propagating fold will have higher horizontal stresses because of the reduced load bearing capacity of the rocks where the fold is growing strongly. In addition the rate of fold growth is slowed in the region of interference where two out-of-phase folds meet as they propagate. This will lead to stress concentrations, increasing the likelihood of fracture.

5. Discussion

The purpose of this paper has been to illustrate that mechanical approaches are necessary in order to make sensible predictions, of not only the large-scale evolution of buckle folds systems but also the distribution of fracture within folded units. Buckle folds are important constituents of compressional belts such as the Zagros mountains of Iran where the stratigraphy consists of alternating competent and incompetent layers. Buckling is likely to be important also in deep water fold belts made up of alternating sand/shale packages.

Our conclusions support traditional views (e.g. Biot, 1961; Ramberg, 1960) where geometric and mechanical evolution of buckle folds relate to the layer thickness and to the relative strength of the layers, as expressed qualitatively as competence. Note that this view contrasts with purely kinematic descriptions of buckle folds (sometimes referred to as detachment folds) where no rock properties are considered (e.g. Mitra, 2002).

Our principal conclusions are those that are consistent with numerous existing empirical results—usually that the hinge curvature has an important influence on fracture and that outer arc fracture is likely to open during buckling. However, the stress history of fold hinges is complex so that while the propensity to fracture is predictable, the timing of those fractures during fold development is not predictable from purely empirical or kinematic approaches. This can be a serious issue for hydrocarbon reservoirs which are charged during fold amplification. Differing failure modes are sensitive to different factors in the stress state of layers. Consequently models are required that make prediction of stress evolution during folding.

Folds develop from a broad, low amplitude perturbation to more localised, pin-jointed type behaviour. This

transition represents a significant reduction in the strength of the folding layer. Consequently the development of folds will impact on the propensity of a rock package to fault. However, at high bulk strains where hinges become tight, the bulk strength increases again, causing the fold deformation to migrate elsewhere or for the folded units to finally fault.

Our study of fold packages on a layer scale has yielded a further series of conclusions. Single isolated folds are likely to have developed from isolated large perturbations. Obvious candidates for these initial features are inherited structures such as early normal faults or abrupt facies changes within competent layers. In contrast, large domains of coherent folds are indications of evenly distributed small initial perturbations.

With large folding rock volumes, the stress state within part of the rock volume is strongly influenced by what is happening around it. This can include the rocks adjacent to rapidly amplifying folds and with folds that propagate into each other. Further investigation is required to examine the role of these larger scale variations on the evolution of local fracture patterns and the prediction of fracture in dynamically evolving systems.

Acknowledgements

This work was supported by Enterprise Oil and by a Natural Environment Research Council ROPA award. This support is gratefully acknowledged. Comments by reviewers Norman Fry and Bernard Colletta are appreciated.

Appendix A

A.1. Finite element analysis

In this appendix some technical details of the finite element methods used are given. The first section describes the modelling of two-dimensional viscous deformations and the way in which finite deformations are built up; the second treats specific aspects of modelling sequences of competent and incompetent layers, and the third covers an extension to a quasi-three-dimensional situation.

A.1.1. Modelling simple two-dimensional fold development

For finite element analysis a simplified abstraction of the natural structure and boundary conditions is used. An example is shown in Fig. A1. The region of the model is subdivided into small elements each of which possesses a set of points called nodes, see Fig. A2. Boundary conditions are based on a constant strain rate being applied to the boundaries and the actual velocities of boundary nodes are calculated from the imposed velocity gradient matrix and the location of the node. The instantaneous deformation is described by the velocities of each of the nodes, which

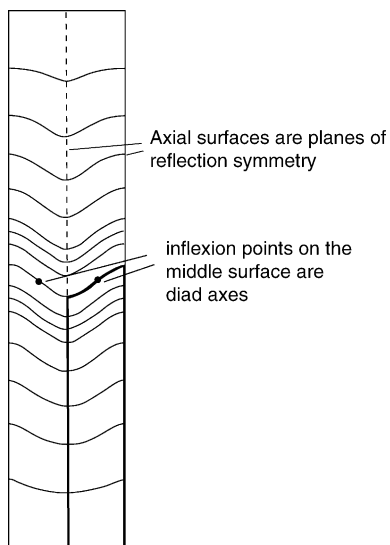


Fig. A1. Schematic diagram of a fold that develops entirely within an anisotropic homogeneous medium. The fold is periodic in the horizontal direction and has an amplitude growing from zero at the top and bottom of the medium to a maximum in the middle. This structure is called an internal buckle.

reduces the infinite number of degrees of freedom in the real fold to a manageable number in the model. The velocities at points within elements are prescribed functions of the values at the nodes. These prescribed functions are polynomials of low degree, quadratic in the case of the elements in Fig. A2. Strain rates can be obtained from the gradients of the velocities and stresses can be obtained from strain rates by application of the rheological equations. For this study a nearly incompressible linear viscosity was used, derived from the equivalent elasticity relations given in Zienkiewicz and Taylor (1994). Isotropic or anisotropic properties are

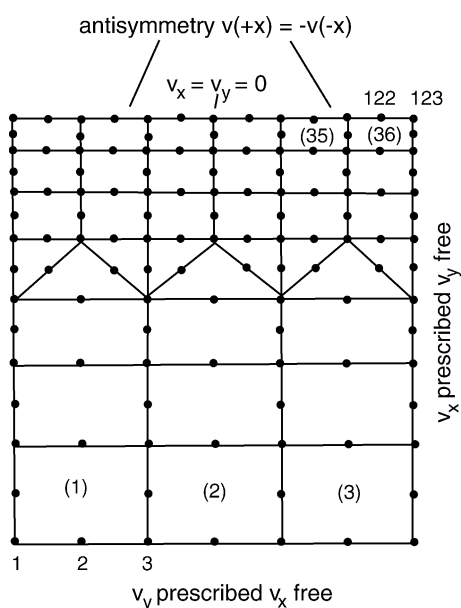


Fig. A2. Example of a finite element mesh used to solve the deformation in an internal buckle.

used as necessary. The finite element method has the advantage that it can find solutions for complex geometries, so that there is no constraint on the fold shapes that may develop. The geometry of the model at any stage in the computation is defined by the coordinate values of the nodes. The finite element solution yields the velocities of the nodes and the velocities are the time rate of change of the coordinates. This means that to follow the evolution of the geometry of the model is to solve a system of ordinary differential equations for the nodal coordinates. The analytical approach shows that the solution is exponential, so the solution method chosen must be able to cope with this sort of solution. A fourth order Runge–Kutta (Conte & De Boor, 1980) method was used. Such a solution method proceeds in time steps, with four finite element solutions per step. The accuracy of the method allows time steps corresponding to large imposed strain increments to be used.

A.1.2. Multilayer folds

A simplification can be made in order to estimate what possible stress variations may be found in the competent layers, as shown in Fig. A3. In this simplification the finite element mesh is set up so that the nodes on the top of the model are in equivalent positions to those on the bottom, and in this case they are in the middle of the incompetent layer, Fig. A3. To maintain a similar profile for this line of nodes the velocities of the top nodes differ by a known amount from those at the bottom. This condition can be used to give the effect of repeating the model in the vertical direction to infinity upwards and downwards. The folds are idealised to have mirror planes of symmetry on the axial plane and points of diad rotational symmetry at the inflexion points of the middle surfaces of the layers. These symmetry conditions can be used to further reduce the portion that needs to be modelled, see the outlined region in Fig. A3. A constant strain-rate was imposed on the boundaries, each finite element solution allows the velocities of nodal points across the finite element mesh to be determined for any geometry of the model, as defined by deformed state coordinates of the mesh. The development of the model as a function of imposed finite strain was calculated using fourth order ordinary differential equation solving methods as above. The step length was a differential logarithmic strain of 0.1. The boundary condition of constant imposed strain rate is an end-member condition. The results were obtained using a multilayer in which each component has the same thickness and the viscosity of the competent units was 10 or 40 times that of the incompetent units. The finite element mesh consisted of 797 nodes and 240 elements. The initial wavelength was 35 times the layer thickness. The initial fold had an amplitude to wavelength ratio of 0.0025, giving a maximum limb dip of 1°.

A.1.3. A quasi-three-dimensional extension

For this part of the study the folds are considered to be similar folds with vertical axial planes, subhorizontal axes,

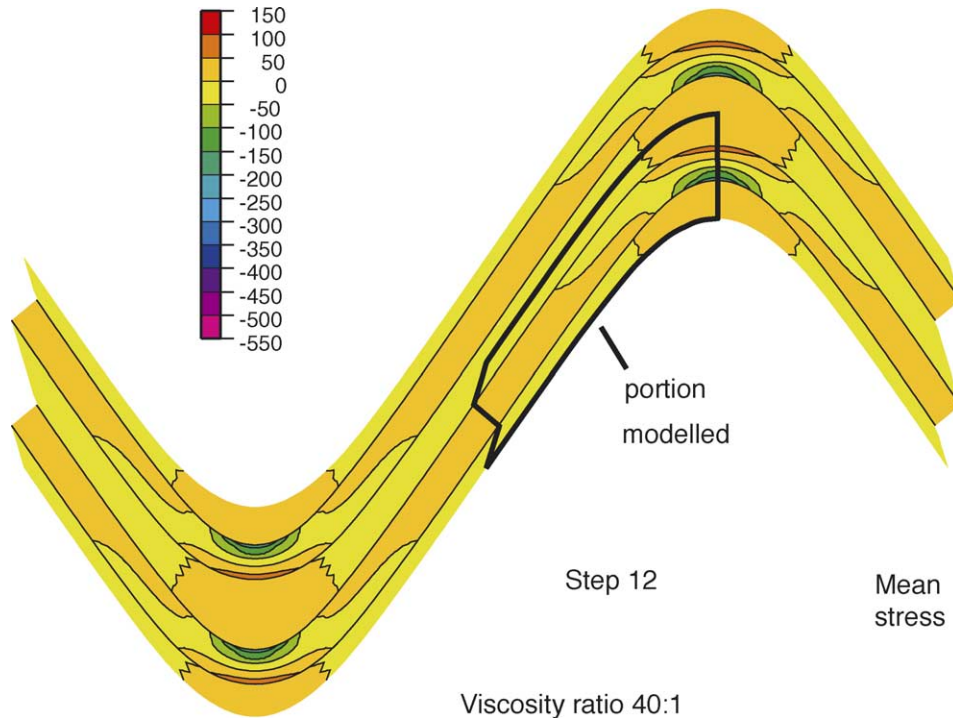


Fig. A3. The value of the mean stress for step 12 in the development of a multilayer similar fold.

and of infinite extent in the vertical direction, forming in a material with anisotropic deformation properties. In this approximation the geometry of the folds can change in the horizontal dimension but folded surfaces separated from one another by vertical displacement have the same geometry, so that a two-dimensional mesh of special elements can be used, one of which is shown in Fig. A4. Each node of the mesh has three degrees of freedom corresponding to the three spatial dimensions, so that the modelled structure can develop effectively in three dimension, subject to the constraint of constant geometry in the vertical direction.

The model used is shown schematically in Fig. A5. It consisted of 501 nodes in 150 eight-node quadrilateral elements and was initially 30 units in the axial direction and 10 units along the folded layers. The initial perturbation was

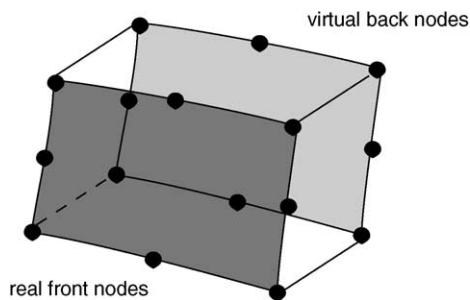


Fig. A4. The element used to model quasi-three-dimensions. The element is an eight-node quadratic element in two dimensions and linear in the third. The condition that geometry remains constant in the third dimension allows the virtual back nodes to be condensed out, leaving an eight-node element with three degrees of freedom per node.

applied as a sine curve of full wavelength with an amplitude of 0.01 at the left hand end of the model and decaying to zero at $x = 10$ units into the model. The decay of amplitude was achieved using a quadratic function with zero slope at $x = 10$. The direction of constant geometry is parallel to z ,

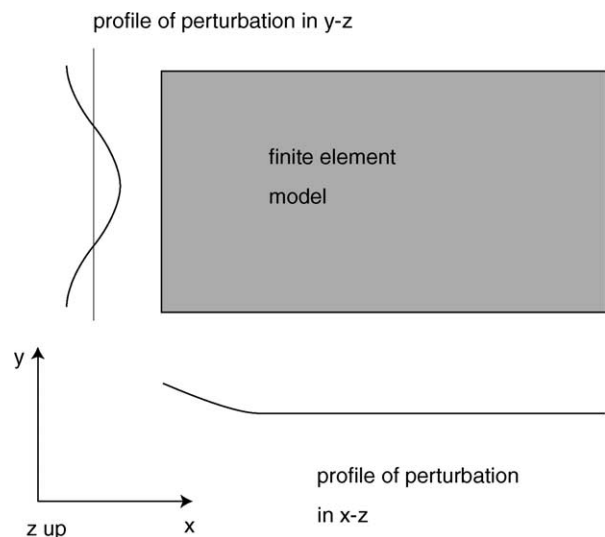


Fig. A5. The finite element model used to investigate along axis fold propagation. The geometry of the folds varies in x - y but is constant in z . An initial perturbation is applied which is shown in y - z section on the left of and in x - z section below the mesh. The perturbation is sinusoidal in y . It is given a small amplitude on the left edge of the model and is made to fall linearly to zero, with continuous slope, after a short distance in x . The top and bottom edges of the model have periodic boundary conditions. The left and right edges of the model are fixed in x and free in y and z . The edges of the model are planes of reflexion symmetry.

so that the folds are similar folds of infinite extent in z . The phase of the initial perturbation could be varied to displace the initial perturbation in y , but always subject to the condition that the point at which $z = 0$ coincided with a node. The boundary conditions on the left hand end were that the nodal displacements (velocities) were fixed in x and free in y and z except that one node with the value of the initial perturbation equal to zero was fixed in all three components. The plane bounding the left-hand of surface of the model had zero shear stress. No constraint was placed on the first derivative of displacement. The centre node of the right hand end of the model was fixed was a centre of inversion symmetry. The nodal displacements above and below the centre node were linked in antisymmetry to give the effect of extending the model a further 30 units to the right with the symmetrically equivalent fold development occurring. The top and bottom of the model were linked with periodic boundary conditions. Appropriate conditions were imposed on the gradient of displacement to ensure continuity.

References

- Biot, M. A. (1961). Theory of folding of stratified viscoelastic media and its implications in tectonics and orogenesis. *Geological Society of America Bulletin*, 72, 1595–1620.
- Biot, M. A. (1965). *Mechanics of incremental deformations*. New York: Wiley.
- Casey, M., & Huggenberger, P. (1985). Numerical modelling of finite-amplitude similar folds developing under general deformation histories. *Journal of Structural Geology*, 7, 103–114.
- Cobbold, P. R. (1975). Fold propagation in single embedded layers. *Tectonophysics*, 27, 333–351.
- Cobbold, P. R. (1977). A finite element analysis of fold propagation—A problematic application. *Tectonophysics*, 38, 339–353.
- Conte, S. D., & De Boor, C. (1980). *Elementary numerical analysis* (3rd ed). New York: McGraw-Hill, 432 pp..
- Cosgrove, J. W., & Ameen, M. S. (2000). A comparison of the geometry, spatial organisation and fracture patterns associated with forced folds and buckle folds. In J. W. Cosgrove, & M. S. Ameen (Eds.), (Vol. 169) (pp. 7–21). *Special Publication of the Geological Society of London*.
- Couples, G. D., & Lewis, H. (1998). Lateral variations of strain in experimental forced folds. *Tectonophysics*, 295, 79–81.
- Dieterich, J. H., & Carter, N. L. (1969). Stress history of folding. *American Journal of Science*, 267, 129–155.
- Ericson, J. B., McKean, H. C., & Hooper, R. J. (1998). Facies and curvature controlled 3D fracture models in a Cretaceous carbonate reservoir, Arabian Gulf. In G. Jones, Q. J. Fisher, & R. J. Knipe (Eds.), *Faulting fracture-sealing and fluid flow in hydrocarbon reservoirs* (Vol. 147) (pp. 213–299). *Special Publication of the Geological Society of London*.
- Fletcher, R. C. (1974). Wavelength selection in the folding of a single layer with power-law rheology. *American Journal of Science*, 274, 1029–1043.
- Hanks, C. L., Lorenz, J., Teufel, L., & Krumhardt, A. P. (1997). Lithologic and structural controls on natural fracture distribution and behavior within the Lisburne Group, northeastern Brooks Range and North Slope subsurface, Alaska. *American Association of Petroleum Geologists Bulletin*, 81, 1700–1720.
- Hennings, P. H., Olson, J. E., & Thompson, L. B. (2000). Combining outcrop data and three-dimensional structural models to characterize fractured reservoirs: An example from Wyoming. *American Association of Petroleum Geologists Bulletin*, 84, 830–849.
- Hunt, G. W., Mühlhaus, H.-B., & Whiting, A. I. M. (1997). Folding processes and solitary waves in structural geology. *Philosophical Transactions of the Royal Society, Series A*, 355, 2197–2213.
- Jamison, W. R. (1997). Quantitative evaluation of fractures on the Monkshood anticline, a detachment fold in the foothills of western Canada. *American Association of Petroleum Geologists Bulletin*, 81, 1110–1132.
- Lisle, R. J. (1992). Constant bed-length folding: Three dimensional geological implications. *Journal of Structural Geology*, 14, 245–252.
- Mancktelow, N. S., & Abbassi, M. R. (1992). Single layer buckle folding in non-linear materials. II. Comparison between theory and experiment. *Journal of Structural Geology*, 14, 105–120.
- Mitra, S. (2002). Structural models of faulted detachment folds. *Bulletin of the American Association of Petroleum Geologists*, 86, 1673–1694.
- Paterson, M. S. (1978). *Experimental rock deformation, the brittle field*. Berlin: Springer, 254 pp..
- Price, N. J., & Cosgrove, J. W. (1990). *Analysis of geological structures*. Cambridge: Cambridge University Press.
- Ramberg, H. (1960). Relationships between length of arc and thickness of pygmatically folded veins. *American Journal of Science*, 258, 36–46.
- Ramsay, J. G. (1967). *Folding and fracturing of rocks*. New York: McGraw-Hill, 568pp.
- Ramsay, J. G. (1974). Development of chevron folds. *Geological Society of America Bulletin*, 85, 1741–1754.
- Satterzedah, Y., Cosgrove, J. W., & Vita Finzi, C. (2000). The interplay between faulting and folding during the evolution of the Zagros deformation belt. In J. W. Cosgrove, & M. S. Ameen (Eds.), *Forced folds and fractures* (169) (pp. 187–196). *Special Publication of the Geological Society of London*.
- Smith, R. B. (1977). Formation of folds, boudinage and mullions in non-Newtonian materials. *Geological Society of America Bulletin*, 88, 312–320.
- Williams, J. R. (1980). Similar and chevron folds in multilayers, using finite element and geometric models. *Tectonophysics*, 65, 323–338.
- Wong, T.-F., David, C., & Zhu, W. (1997). The transition from brittle faulting to cataclastic flow in porous sandstones: Mechanical deformation. *Journal of Geophysical Research*, 102, 3009–3025.
- Zienkiewicz, O. C., & Taylor, R. L. (1994). *The finite element method* (4th ed). New York: McGraw-Hill.